



Siedlce University
of Natural Sciences
and Humanities



On Delay Time Problem of Galactic Cosmic Rays - Experimental and Theoretical Study

Marek Siluszyk^{1,2}, Krzysztof Iskra²,

1. Siedlce University of Natural Sciences and Humanities, Siedlce, Poland

2. Polish Air Force University, Deblin, Poland

Abstract

We study modulation of Galactic Cosmic Rays (GCR) particles based on the Parker's Transport Equation, which describe a four major processes: convection, diffusion, drift and adiabatic cooling responsible for modulation of the GCR flux.

We taking into account the physical parameters characterizing the GCR modulation in the interplanetary space; as radial and tangential components of the GCR anisotropy in various sectors of the heliospheric magnetic field (HMF) and module B of the HMF and changes of drift effect of the GCR particles with solar activity (SA). Our approach is the implementation of two independent parameters (proxies), γ and v in different periods of SA.

The solutions of numerical model are compared with the variations of the GCR measured by NMs. We show the existence of a changing delay time (DT) between the changes of GCR intensity and the parameters characterizing SA. We obtained different DTs in considered Solar Cycles from 20 to 23.

We conclude that the calculated DT is compared with observed DT and is a very significant parameter for study modulation of GCR.

Introduction

Many studies of the DT problem showed that DTs are more pronounced in odd-numbered cycles (Burlaga, McDonald, and Ness, 1993; Parker, 1963) than in even-numbered cycles (Jokipii and Thomas, 1981). Scientists explain this phenomenon by drift effects (Cliver and Ling, 2001; Chowdhury, Kudela, and Dwivedi, 2013; Chowdhury and Kudela, 2018; Mavromichalaki, Belehaki, and Rafio, 1998). Based on the drift theory (Jokipii, 1971) of modulation of GCR in solar cycles with $A > 0$, where A is the polarity state of the solar magnetic field, a drift stream of GCR caused by the gradient and curvature of the IMF preferentially enters the heliosphere from the polar region and is ejected outward along the equatorial current sheet. The reverse situation occurs in periods when $A < 0$, the drift stream of GCR enters the heliosphere along of the heliospheric current sheet (HCS) and leaves it near the poles of the Sun. In periods when $A < 0$, GCR particles are more affected by propagating diffusive barriers associated with SA and the waviness of the HCS, resulting in large DTs. The opposite situation is observed in periods with $A > 0$. GCR particles are less affected by propagating diffusive barriers which cause small DTs or no DTs.

GEOPHYSICAL RESEARCH LETTERS, VOL. 27, NO. 16, PAGES 2453-2456, AUGUST 15, 2000

On the modulation of galactic cosmic ray intensity during solar activity cycles 19, 20, 21, 22 and early 23

James A. Van Allen

Solar Physics (2022) 297:38
<https://doi.org/10.1007/s11207-022-01970-1>



Time Lag Between Cosmic-Ray and Solar Variability: Sunspot Numbers and Open Solar Magnetic Flux

Sergey A. Koldobskiy^{1,2} · Riikka Kähkönen¹ · Bernhard Hofer³ · Natalie A. Krivova³ · Gennady A. Kovaltsov^{2,4} · Ilya G. Usoskin¹

THE ASTROPHYSICAL JOURNAL LETTERS, 849:L32 (6pp), 2017 November 10

© 2017. The American Astronomical Society.

OPEN ACCESS

<https://doi.org/10.3847/2041-8213/aa9373>



Evidence for a Time Lag in Solar Modulation of Galactic Cosmic Rays

Nicola Tomassetti¹ , Miguel Orcinha² , Fernando Barão² , and Bruna Bertucci¹

Solar Physics (2022) 297:113
<https://doi.org/10.1007/s11207-022-02048-8>



Extracting Hale Cycle Related Components from Cosmic-Ray Data Using Principal Component Analysis

Jouni Takalo¹

Received: 31 January 2022 / Accepted: 3 August 2022
© The Author(s) 2022



Modeling the Time Delay Problem of Galactic Cosmic Ray Flux in Solar Cycles 21 and 23

M. Siluszyk^{1,2} · K. Iskra¹

To model the 11-year variations of GCRs we use a non-stationary PTE (Parker, 1965; Manuel, Ferreira, and Potgieter, 2014).

$$\frac{\partial N}{\partial \tau} = -(U + \langle v_d \rangle) \cdot \nabla N + \nabla \cdot (K_{ij}^S \cdot \nabla N) + \frac{1}{3} (\nabla \cdot U) \frac{\partial N}{\partial \ln R_i}$$

where N , R , τ , U , v_d are the omnidirectional distribution function, the rigidity of the CR particles, the time, the SW speed, and the drift velocity, respectively.



Experimental Investigation of the Delay Time in Galactic Cosmic Ray Flux in Different Epochs of Solar Magnetic Cycles: 1959 – 2014

Krzysztof Iskra¹ · Marek Siluszyk² · Michael Alania^{2,3} · Witold Wozniak⁴

Table 3 Correlation coefficients, r , and DTs for 10 sub-periods. In the cycles column, upward and downward arrows represent ascending and descending GCR intensity, respectively (see text and Table 2).

No	Period	Cycles	$r(\text{SSN}, I_{\text{GCR}})$	DT (SSN, I_{GCR}) [months]	$r(\text{SSN}, B)$	DT (SSN, B) [months]	$r(\text{SSN}, \text{TA})$	DT (SSN, TA) [months]	$r(B, I_{\text{GCR}})$	DT (B, I_{GCR}) [months]	$r(B, \text{TA})$	DT (B, TA) [months]	$r(\text{TA}, \text{GCR})$	DT (TA, GCR) [months]
1	1959–1965	19 A < 0 ↗	0.91	15–16	–	–	–	–	–	–	–	–	–	–
2	1965–1968	20 A < 0 ↘	0.88	5	–	–	–	–	–	–	–	–	–	–
3	1971–1976	↗ A > 0	0.40	0	0.46	–	–	–	–0.53	1	–	–	–	–
4	1976–1978	21 ↘ A > 0	0.84	1	0.86	1	0.98	0	–0.92	0	0.87	13	–0.93	3
5	1981–1987	A < 0 ↗	0.87	10–11	0.84	5	0.90	4	–0.81	0	0.86	–2	–0.93	4
6	1987–1988	22 A < 0 ↘	0.96	4–5	0.88	–7	0.97	0	–0.68	0	0.94	17	–0.97	10
7	1991–1997	↗ A > 0	0.92	0	0.96	2	0.96	–13	–0.88	0	0.91	–14	–0.97	5
8	1997–1999	23 ↘ A > 0	0.86	4–5	0.91	–9	0.93	–1	–0.80	1	0.72	8	–0.97	12
9	2002–2009	A < 0 ↗	0.93	13–14	0.93	13	0.91	2	–0.94	0	0.95	–4	–0.94	3
10	2009–2013	24 A < 0 ↘	0.80	1	0.85	–5	0.92	–11	–0.84	1	0.86	–4	–0.89	5

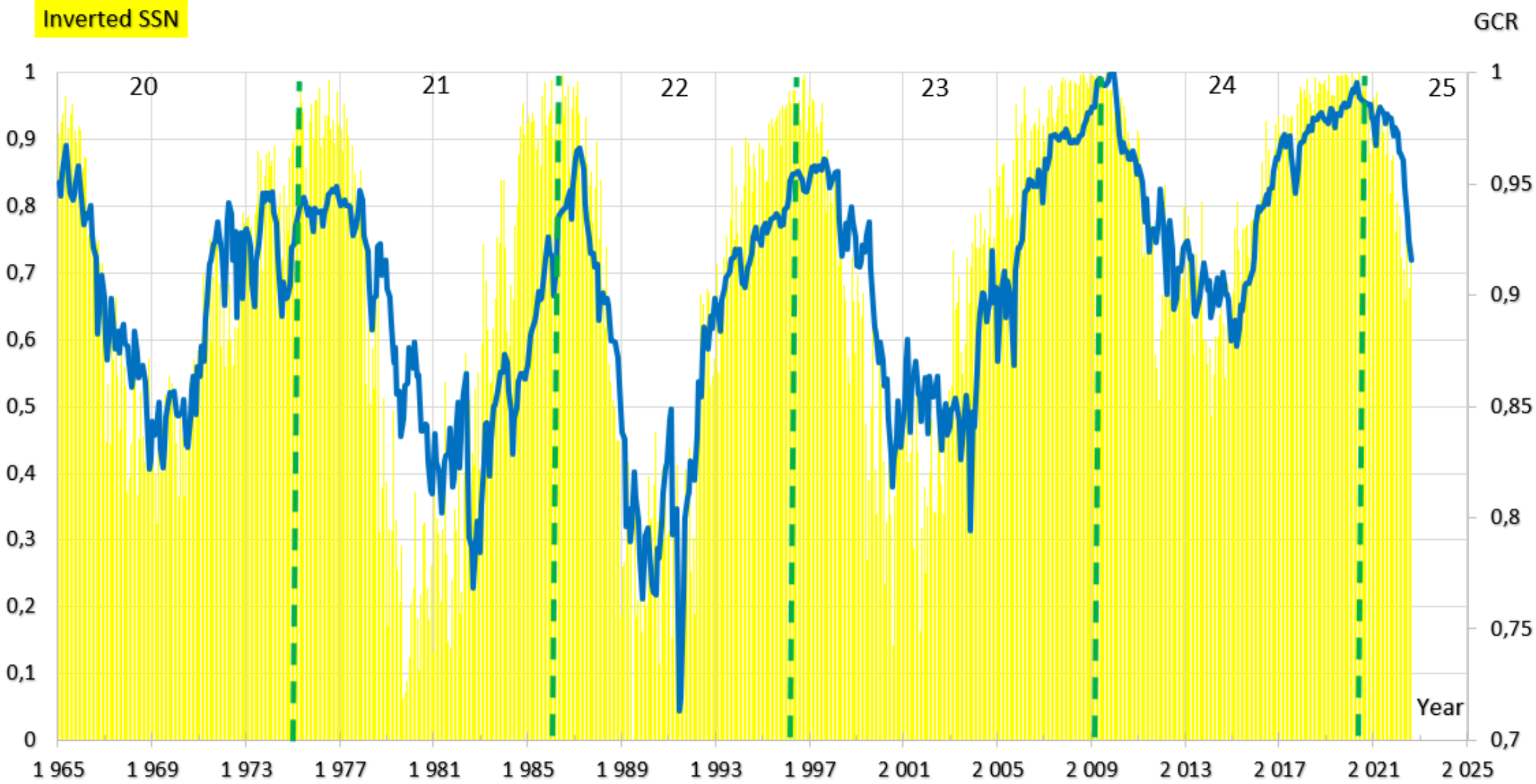


Figure
Temporal changes of the normalized monthly intensity of the GCR observed by the Oulu NM versus inverted SSN.

I. Theoretical Study

The long period variation of the Galactic Cosmic Ray (GCR) flux can be interpreted based on the diffusion-convection model [1]. The diffusion flux plays a main role together with fluxes of convection and adiabatic cooling in formation of the long period variation of the GCR intensity [2]. Nevertheless, an acceptance of this assumption requires an answer to an important question, **what parameter or group of parameters characterized solar activity (SA) and solar wind (SW) are responsible for the changes of diffusion of the GCR particles.** To response to this question we have to consider other all possible arguments being in our disposition. The first one is a parameter γ which characterises the temporal changes of the power law rigidity R spectrum of GCR flux variation given by a formula ,

$$\frac{\delta D(R)}{D(R)} \propto R^{-\gamma}$$

The second parameter is an exponent ν of the Power Spectral Density (PSD) of the Heliospheric Magnetic Field (HMF) turbulence ($PSD \propto f^{-\nu}$, f is frequency) [3].

Hence, we have two very important physically realistic parameters γ and ν calculated from the independent sources. Solution of PTE obtained in numerical investigation are compared with data of the GCR flux measured by Oulu NM. So, the both autonomous parameters γ and ν can be considered as the crucial indicators to study GCR propagation in heliosphere [4, 5]. We have found a strong inversely correlation between γ and ν in considered solar cycles 20, 21, 22 and 23 [6].

To estimate a role of changes of diffusion coefficient in the long period changes of the GCR flux registered by NMs we consider a parallel diffusion coefficient $k_{||}$ having a form [7, 8]:

$$k_{||} = C \cdot R^{\alpha}$$

where,

$$C = \frac{c\beta\nu(\nu+2)B^{\nu}}{9A}$$

Power Spectral Density (PSD) of the IMF's turbulence

$$PSD \propto f^{-\nu}$$

ν

$$\alpha = 2 - \nu$$

$$\nu = -1.04\gamma + 2.06$$

The rigidity spectrum exponent the isotropic intensity variations of GCR

α

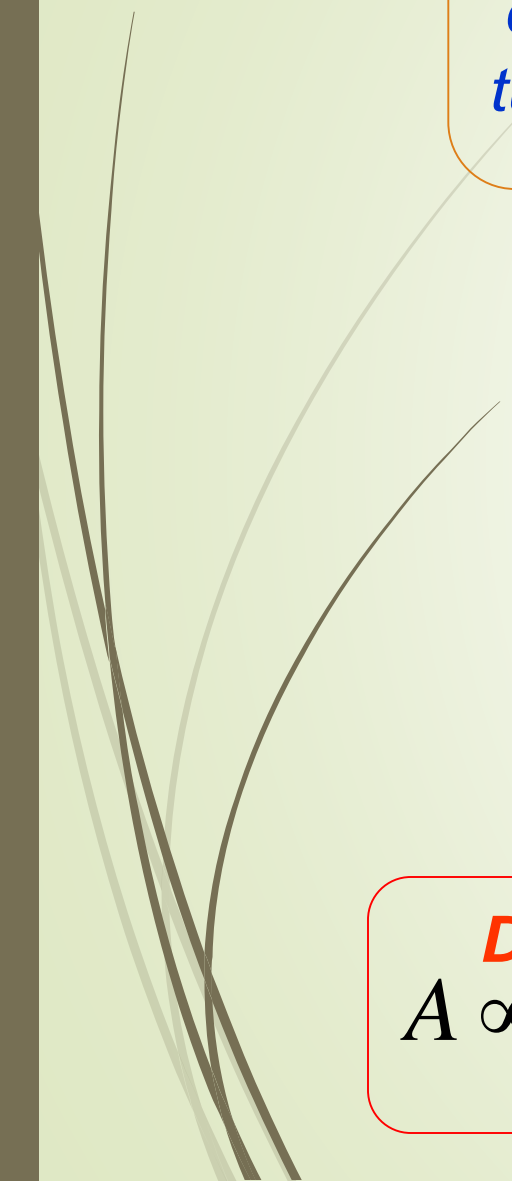
$$\gamma(\alpha) = 0.96 \cdot \alpha + 0.06$$

γ

Diffusion

$$A \propto \frac{1}{K_{\parallel}} \propto \frac{1}{R^{\alpha}}$$

$$\frac{\delta D(R)}{D(R)} \propto \frac{1}{R^{\gamma}}$$



An important phenomenon in cosmic ray modulation (which is observed at earth orbit) is a 'Delay Time' (DT) between temporal changes of time profiles of the GCR intensity I and any parameters of SA and SW, e.g., sunspot numbers (SSN), SW velocity, interplanetary magnetic field strength (B) and others during the 11-year period of SA. We call DT a time interval between extremes of the GCR intensity I changes on the one side and any parameters of SA and SW on the other.

As a rule we examine one to one correspondence between maximum value of GCR intensity and minimum value of any parameters of SA and SW. Generally, to model PTE describing a propagation of energetic GCR particles is a reasonably difficult problem due to complexity of electromagnetic processes in the heliosphere. These processes are well reflected in symmetric and asymmetric parts of 3-D generalised anisotropic tensor of GCR diffusion [Alania, 1978].

$$\begin{aligned}
 K_{11} &= K_{II} \left[\cos^2 \delta \cos^2 \psi + \beta (\cos^2 \delta \sin^2 \psi + \sin^2 \delta) \right] & K_{21} &= K_{II} \left[\sin \delta \cos \delta \cos^2 \psi (1 - \beta) + \beta_1 \sin \psi \right] & K_{31} &= K_{II} \left[\cos \delta \sin \psi \cos \psi (\beta - 1) + \beta_1 \sin \delta \cos \psi \right] \\
 K_{12} &= K_{II} \left[\sin \delta \cos \delta \cos^2 \psi (1 - \beta) - \beta_1 \sin \psi \right] & K_{22} &= K_{II} \left[\sin^2 \delta \cos^2 \psi + \beta (\sin^2 \delta \sin^2 \psi + \cos^2 \delta) \right] & K_{32} &= K_{II} \left[\sin \delta \sin \psi \cos \psi (\beta - 1) - \beta_1 \cos \delta \cos \psi \right] \\
 K_{13} &= K_{II} \left[\sin \psi \cos \delta \cos \psi (\beta - 1) - \beta_1 \sin \delta \cos \psi \right] & K_{23} &= K_{II} \left[\sin \delta \sin \psi \cos \psi (\beta - 1) + \beta_1 \cos \delta \cos \psi \right] & K_{33} &= K_{II} \left[\sin^2 \psi + \beta \cos^2 \psi \right]
 \end{aligned}$$

where,

$\psi = \arctan(-B_\phi / B_r)$ - the angle between the lines of the HMF and the radial direction in the meridian plane

$\delta = \arctan(B_\theta / B_r)$ - the angle between the radial direction and HMF lines in the equatorial plane

Mathematical modelling: long period variation of GCR: 1976 – 1987 and 1997 – 2009

Our aim is to compare results of modelling of GCR transport for 11-year solar cycles #21 and #23. Those cycles were chosen because of both consists from the similar polarities of the ascending ($A>0$) and descending ($A<0$) epochs of the 11-year cycle of SA. Moreover, in considered cycles are observed pure inverse correlation between the temporal changes of the rigidity spectrum exponent γ and the exponent ν of the PSD of the HMF turbulence. Our previous papers [10, 11] show that the turbulence of the HMF have a Gaussian distribution and the GCR particles propagation can be considered as normal diffusion. To model the 11-year variations of GCRs we use non-stationary PTE [12, 13].

$$\frac{\partial N}{\partial \tau} = -(\mathbf{U} + \langle \mathbf{v}_d \rangle) \cdot \nabla N + \nabla \cdot (\mathbf{K}_{ij}^S \cdot \nabla N) + \frac{1}{3} (\nabla \cdot \mathbf{U}) \frac{\partial N}{\partial \ln R_i} \quad (1)$$

where N and R are the omnidirectional distribution function and rigidity of the GCR particles, respectively; τ – the time, U – the solar wind velocity and v_d is the drift velocity.

We set up the dimensionless density $f = \frac{N}{N_0}$, the time $t = \frac{\tau - \tau_0}{\tau_s - \tau_0}$ and rigidity $R = \frac{R_i}{1 \text{ GeV}}$ and the distance

$r = \frac{\rho}{\rho_0}$; N_0 is the density in the Local Interstellar Medium (LISM) accepted as $N_0 = 4\pi I_0$, where the

intensity I_0 in the LISM has the form: $I_0 = 21.1 T^{-2.8} / (1 + 5.85 T^{-1.22} + 1.18 T^{-2.54})$ in [14, 15]; T is kinetic energy in GeV ($T = \sqrt{R^2 \cdot e^2 + 0.938[\text{GeV}]^2} - 0.938[\text{GeV}]$), e is an elementary electric charges, ρ and ρ_0 are the radial distance and size of the modulation region; τ_0 – is the characteristic time corresponding to the changes in the heliosphere for the certain class of the GCR variation.

The size of the modulation region $\rho_0 = 100 \text{ AU}$, and the solar wind velocity $U = 400 \text{ km} \cdot \text{s}^{-1}$ is used throughout the heliosphere. After transformation the equation (1) with the dimensionless variables f , t and R in the 2-D spherical coordinate system (r, θ) can be written, as:

$$A_1 \frac{\partial^2 f}{\partial r^2} + A_2 \frac{\partial^2 f}{\partial \theta^2} + A_3 \frac{\partial^2 f}{\partial r \partial \theta} + A_4 \frac{\partial f}{\partial r} + A_5 \frac{\partial f}{\partial \theta} + A_6 f + A_7 \frac{\partial f}{\partial R} = A_8 \frac{\partial f}{\partial t} \quad (2)$$

where coefficients $A_i(r, \theta, R, t)$ for $i=1, 2, \dots, 8$ are functions, as.

$$A_1 = \chi_{rr}$$

$$A_2 = \frac{\chi_{\theta\theta}}{r^2}$$

$$A_3 = \frac{(\chi_{r\theta} + \chi_{\theta r})}{r}$$

$$A_4 = 2 \frac{\chi_{rr}}{r} + \frac{1}{r} \text{ctg}\theta \chi_{\theta r} + \frac{1}{K_{\parallel}} \frac{\partial K_{rr}}{\partial r} + \frac{1}{r} \frac{1}{K_{\parallel}} \frac{\partial K_{\theta r}}{\partial \theta} - r_0 \frac{1}{K_{\parallel}} U$$

$$A_5 = \frac{1}{r^2} \chi_{r\theta} + \frac{1}{r^2} \text{ctg}\theta \chi_{\theta\theta} + \frac{1}{r} \frac{1}{K_{\parallel}} \frac{\partial K_{r\theta}}{\partial r} + \frac{1}{r^2} \frac{1}{K_{\parallel}} \frac{\partial K_{\theta\theta}}{\partial \theta}$$

$$A_6 = -3 r_0 \frac{1}{r} \frac{1}{K_{\parallel}} \left(U + \frac{1}{2} r \frac{\partial U}{\partial r} \right)$$

$$A_7 = \frac{2}{3} R r_0 \frac{1}{r} \frac{1}{K_{\parallel}} \left(U + \frac{1}{2} r \frac{\partial U}{\partial r} \right)$$

$$A_8 = \frac{r_0^2}{t_0 * K_{\parallel}}$$

The anisotropic diffusion tensor of GCR has a form $K_{ij} = K_{ij}^{(S)} + K_{ij}^{(A)}$ and consists of the symmetric $K_{ij}^{(S)}$ and $K_{ij}^{(A)}$ – antisymmetric parts. We implement a drift velocity of the GCR particles in the model as,

$\langle v_{D,i} \rangle = \frac{\partial K_{ij}^{(A)}}{\partial x_j}$ [16]. This expression is equivalent to the standard formula for $\langle v_D \rangle$ [17]. So, as an ad

hoc assumption we employ the ratios of the perpendicular K_{\perp} and drift K_d diffusion coefficients to the parallel K_{\parallel} diffusion coefficient $\beta = \frac{K_{\perp}}{K_{\parallel}}$ and $\beta_1 = \frac{K_d}{K_{\parallel}}$ for the cosmic ray particles of rigidities $R \geq 10$ GV, as

follows,

$$\beta = \frac{1}{1 + \omega^2 \tau_1^2}, \quad \beta_1 = \frac{\omega \tau_1}{1 + \omega^2 \tau_1^2}, \quad (3)$$

where for rigidities $R=10$ GV is accepted that e.g. at the earth orbit $\omega \tau_1=3$, i.e. $\beta=0.1$. Then, changes of $\omega \tau_1$ is determined by the Parker's spiral magnetic field in the whole heliosphere. The Quasi Linear Theory (QLT) expressed energy/rigidity dependence as, $K(R) \propto R^{\alpha}$ (see equation (1)), where α is diffusion parameter, which is valid for rigidities $R > 10$ GV [7, 18, 19, 20]. We show (see Figure 3) that both proxies γ and v adequately can be used to describe state of heliosphere. Hence, based on the equation (2) we construct two different models for both proxies (there is 8|cases).



$$K_{||} = K_0(r, \theta, \varphi, R, t, \dots?)$$

$$K(r, R) = K(r) \cdot K(R)$$

$$K_{||} = K_0 \cdot K(r) \cdot K(R)$$

$$K_{II} = K_0 \cdot K(r) \cdot K(t) \cdot K(R, \nu(t))$$

$$K_{II} = K_0 \cdot K(r) \cdot K(t) \cdot K(R, \gamma(t))$$



Model I: We used as a proxy parameter γ , where a parallel diffusion coefficient is expressed, as:

$$K_{II} = K_0 K(r) K(t) K(R, \gamma(t)), \quad (4)$$

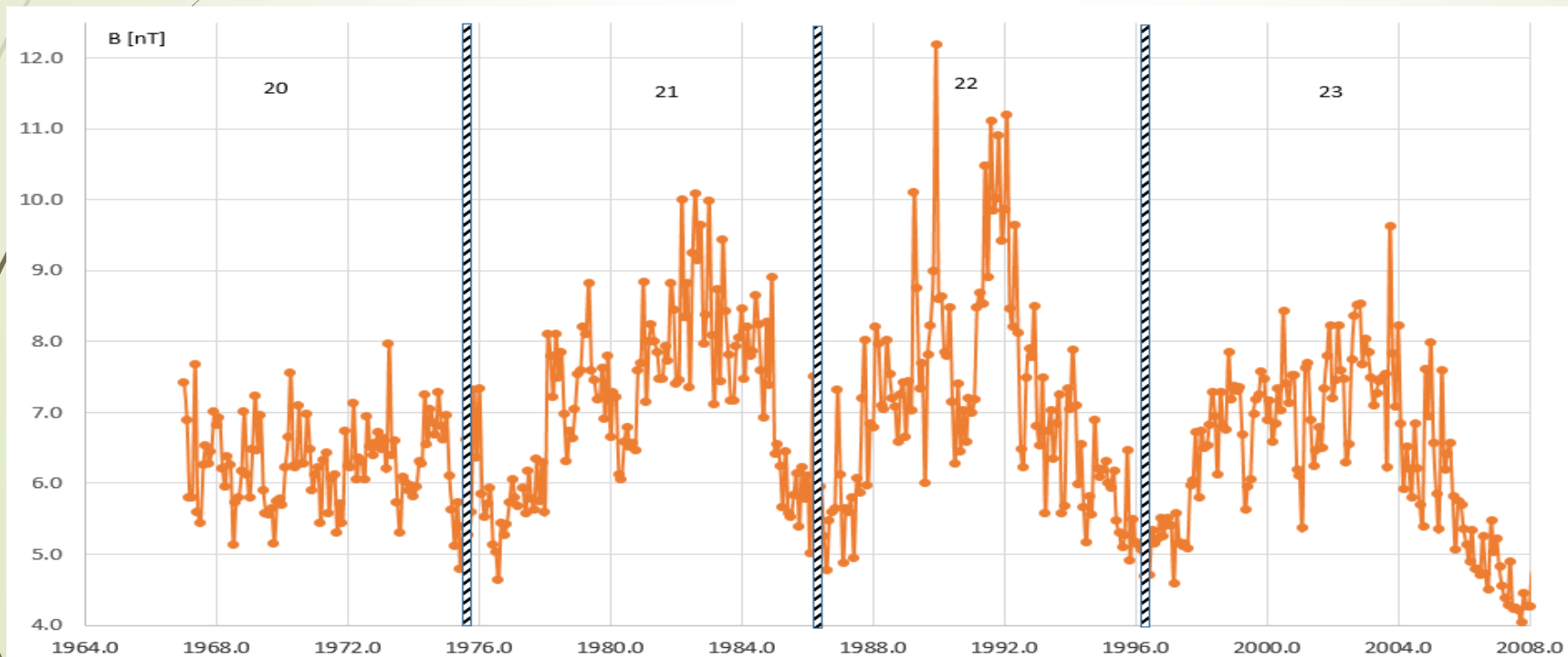
The term describing energy/rigidity dependence has a form $K(R, \gamma(t)) = R^{\gamma(t)}$

Model II: We construct model using the parameter ν , where parallel diffusion coefficient is expressed, as:

$$K_{II} = K_0 K(r) K(t) K(R, \nu(t)), \quad (5)$$

The term describing energy/rigidity dependence is $K(R, \nu(t)) = R^{\nu(t)}$.

Others components are $K_0 = 1.9 \times 10^{19} \text{ cm}^2 / \text{s}$, $K(r) = 1 + 50r$. The function $K(t)$ is introduced to make a consistent change of the diffusion coefficient K_{II} throughout the solar magnetic cycle.

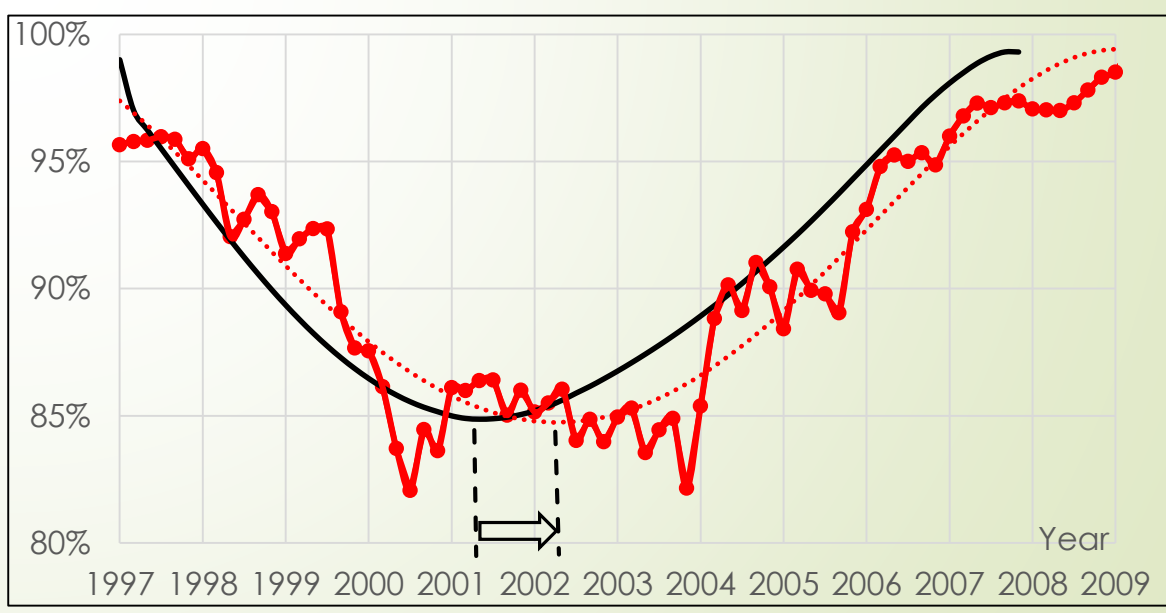
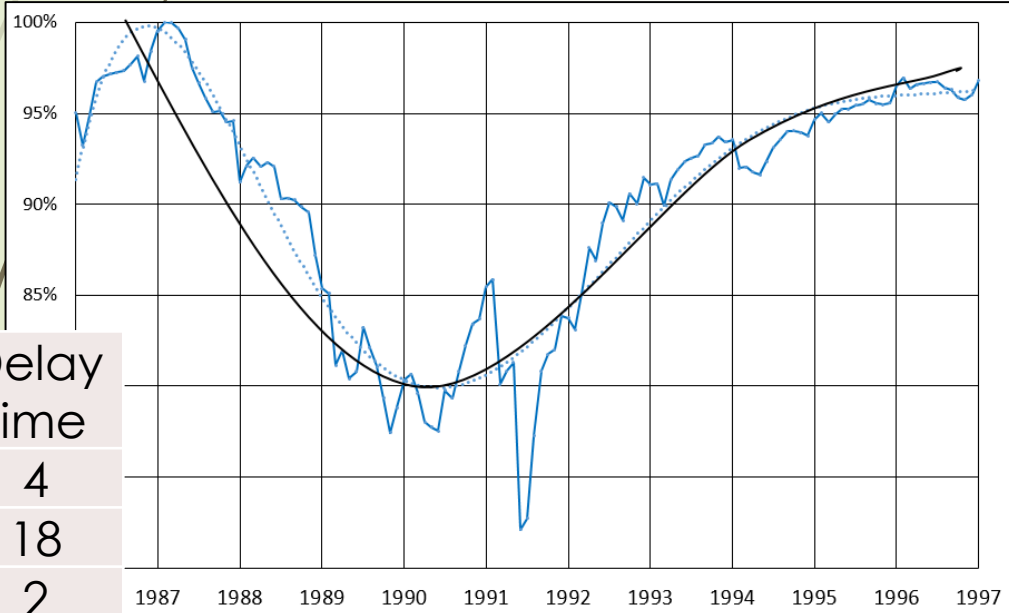
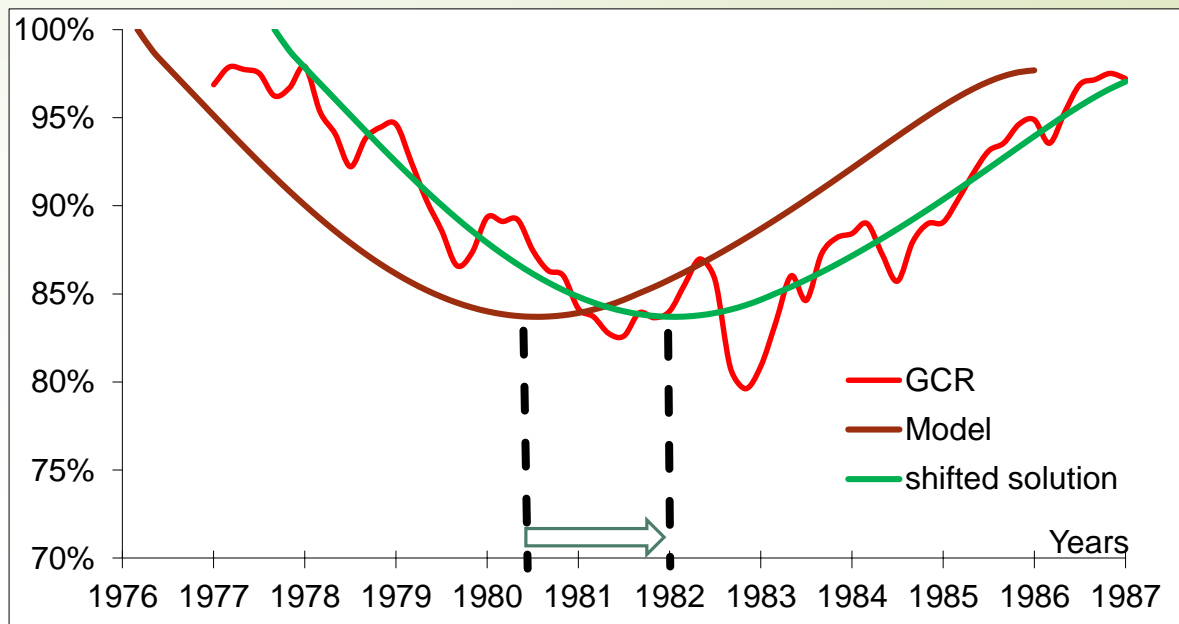
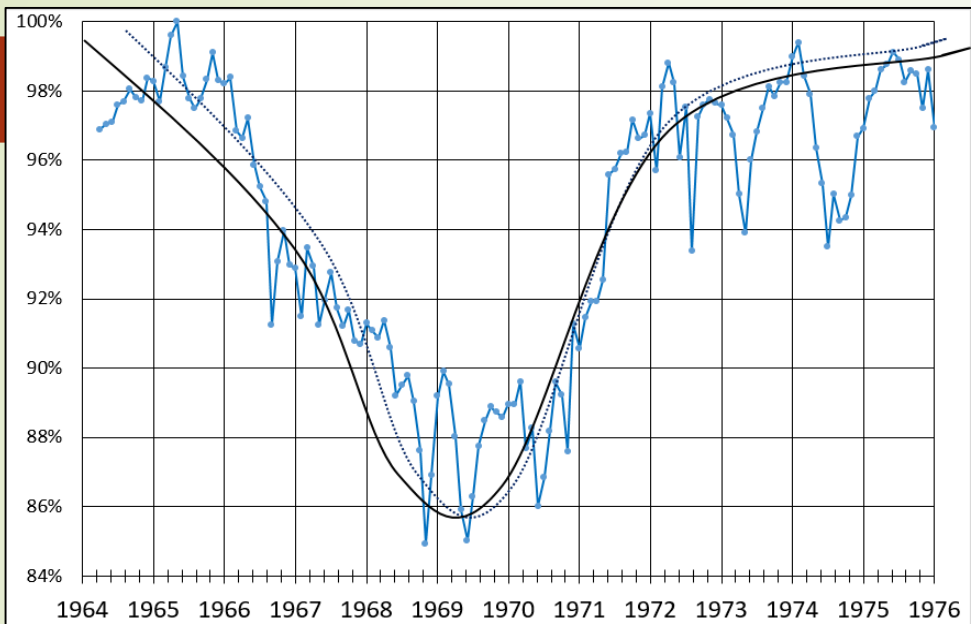


Modeling the Time Delay Problem of GCR Flux

Table 1 The functions implemented in the models for Solar Cycles 21 and 23.

Functions	Period I, 1976–1987, Solar Cycle 21	Period II, 1997–2009, Solar Cycle 23
γ	$\gamma(t) = \sin(\pi \cdot t) + 0.37$	$\gamma(t) = -0.0097 \cdot t^2 + 0.1011 \cdot t + 0.7149$
ν	$\nu(t) = 1.0738 \cdot t^2 - 0.6844 \cdot t + 1.567$	$\nu(t) = 0.0088 \cdot t^2 - 0.1198t + 1.8149$
Normalized parallel coefficient	$K(t) = 2.3 \cdot \exp(4 \cdot t)$	$K(t) = \exp(4.6 \cdot (1.07t^2 - 0.68 \cdot t + 1.57))$
B	$B(t) = -10.35 \cdot t^2 + 10.29 \cdot t + 5.04$	$B(t) = -9.45 \cdot t^2 + 8.04 \cdot t + 5.73$
Drift ratio	$D(t) = 3.2 \cdot t^2 - 3.2 \cdot t + 1.0$	$D(t) = 4.0 \cdot t^2 - 4.0 \cdot t + 1.0$
Tilt angle	$\delta(t) = 408.6 \cdot t^3 - 759 \cdot t^2 + 360.7 \cdot t - 1.4$	$\delta(t) = -140.98 \cdot t^2 + 125.63 \cdot t - 19.759$

RESULTS:



Solar cycle	Delay time
20	4
21	18
22	2
23	12

CONCLUSIONS:

1. The new 2-D time dependent models of the 11-year variation was developed. This model implements the physical parameters characterizing the temporal changes of the magnitude B of the IMF, TA of the HNS, parameters obtained from anisotropy and parameters: γ and ν for the 4 solar cycles: from #20 to #23.
2. In the models temporal changes of the rigidity spectrum exponent γ , characterizing a rigidity dependence of amplitudes of the 11-year variations of the GCR intensity, and the exponent ν of the PSD of the HMF turbulence were implemented as proxies.
3. The temporal changes of the physical parameters implemented in the 2-D model have different delay times with respect to the temporal changes of the smoothed experimental data of the GCR intensity observed by NM Oulu.
4. We obtained different DT for the SC: from #20 to #23
- an acceptable compatibility is kept when the minimum of the expected temporal changes of the GCR particles density is shifted with respect to the minimum of the temporal changes of the smoothed experimental data of the GCR intensity.

Solar cycle	from	to	Delay time
20	1964	1976	4
21	1976	1986	18
22	1986	1996	2
23	1996	2008	12

II. Experimental Study

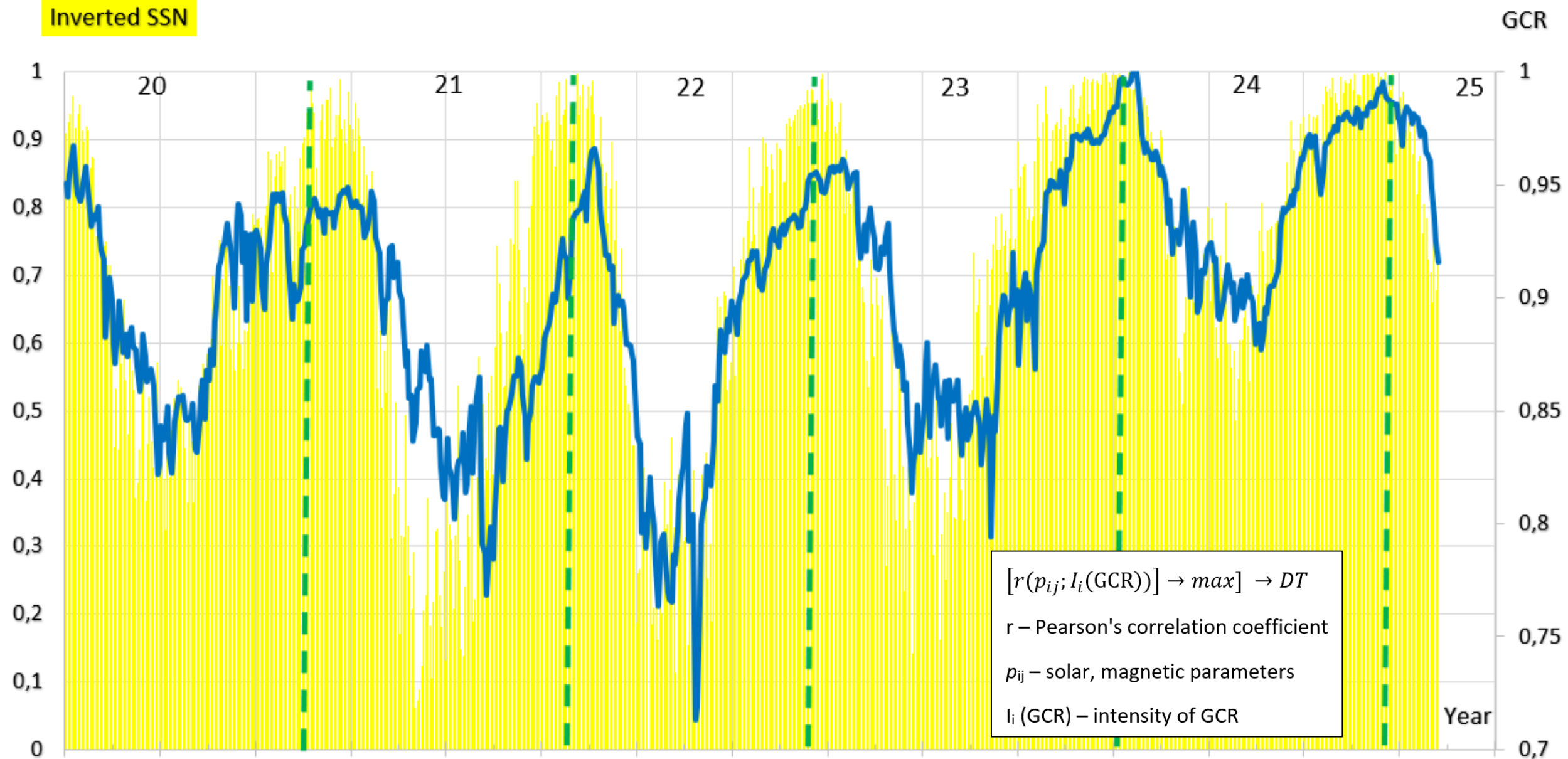


Figure
Temporal changes of the normalized monthly intensity of the GCR observed by the Oulu NM versus inverted SSN.

We analyze five sub-periods with different global solar magnetic field (GSMF) polarities in the period 1959–2014. In the time profile of the GCR intensity, we can observe a plateau for the positive polarity ($A > 0$) and a peak for the negative polarity ($A < 0$) of the GSMF. This is caused by a drift occurring due to the gradient and curvature of the regular interplanetary magnetic field (IMF) (Jokipii and Thomas, 1981). Lockwood and Webber (1984) have suggested that the 11-year variation in GCRs depends on the accumulative effects of Forbush decreases. Others have tried to explain the 11-year variation as a result of a combination of drift and globally merged interaction regions with a time-dependent model (Le Roux and Potgieter, 1995), or by the diffusion barrier with other general modulation mechanisms (Ferreira and Potgieter, 2004). In several articles (Alania *et al.*, 2001; Alania, Iskra, and Siluszyk, 2003, 2008a,b, 2010; Siluszyk *et al.*, 2005; Siluszyk, Iskra, and Alania, 2014; Iskra, Siluszyk, and Alania, 2015; Siluszyk *et al.*, 2018) researchers have shown that large-scale structural changes of the solar wind (SW) magnetic turbulence in different periods of SA are general mechanisms of the 11-year variations of GCR.

$$[r(p_{ij}; I_i(\text{GCR}))] \rightarrow \max] \rightarrow DT$$

r – Pearson's correlation coefficient

p_{ij} – solar, magnetic parameters

$I_i(\text{GCR})$ – intensity of GCR

Number of shifted months i	1959–1969 $r(\text{SSN}, I_i(\text{GCR}))$	1991–1999 $r(\text{SSN}, I_i(\text{GCR}))$
0	-0.62	-0.88
1	-0.65	-0.88
2	-0.68	-0.90
3	-0.71	-0.92
4	-0.74	-0.94
5	-0.76	-0.94
6	-0.78	-0.93
7	-0.80	-0.91
8	-0.81	-0.88
9	-0.82	-0.84
10	-0.84	-0.79
11	-0.85	-0.76
12	-0.86	-0.73
13	-0.87	-0.70
14	-0.88	-0.66
15	-0.89	-0.63
16	-0.89	-0.59
17	-0.89	-0.55
18	-0.88	-0.52
19	-0.87	-0.48
20	-0.86	-0.45
21	-0.85	-0.42
22	-0.84	-0.39
23	-0.83	-0.36
24	-0.80	-0.33

The correlation coefficient, r , between monthly data of the GCR flux and each of the SA parameters, SSN, TA, and B, was calculated for the considered periods, with various monthly shifts: $\Delta t = 0, 1, 2, \dots, 18$ months, to study the DT.

For instance, we calculated the correlation coefficient, for two independent series of input data of SSN and GCR. Next, $I(\text{GCR})$ data was shifted in $0, 1, 2, \dots, 18$ monthly steps

$$[r(p_{ij}; I_i(\text{GCR}))] \rightarrow \max] \rightarrow DT$$

r – Pearson's correlation coefficient

p_{ij} – solar, magnetic parameters

$I_i(\text{GCR})$ – intensity of GCR

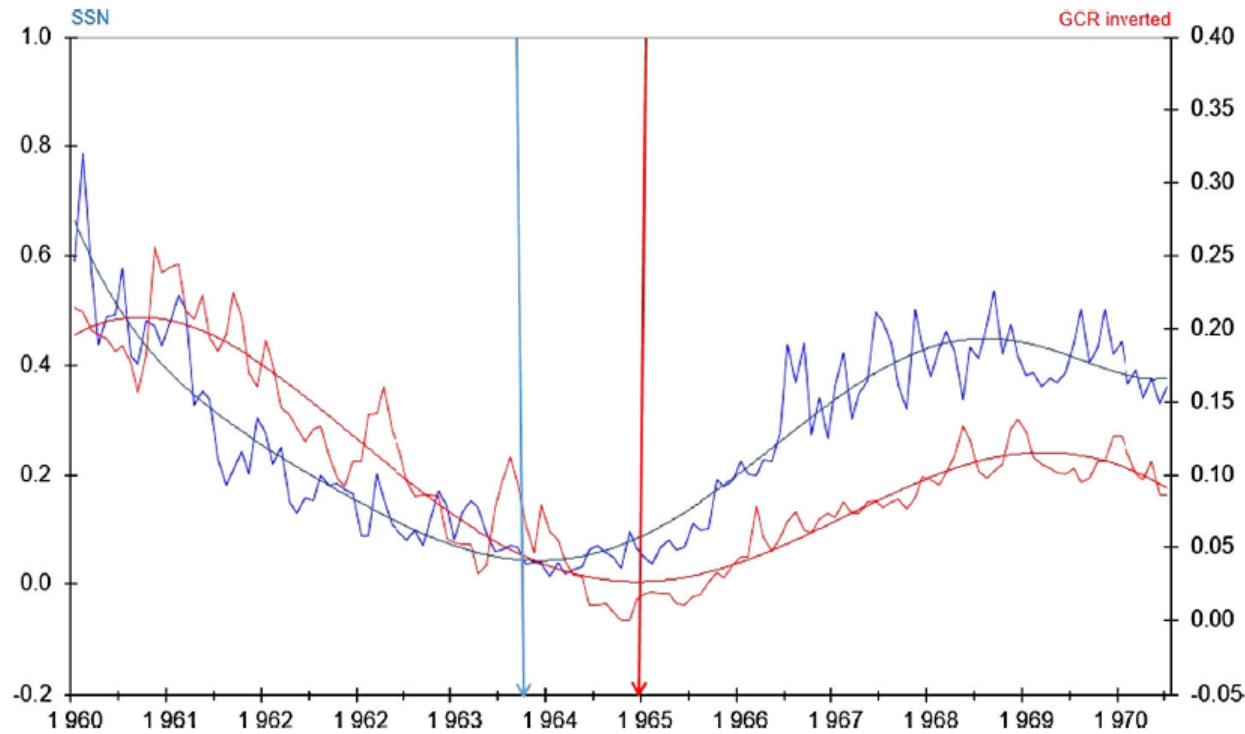


Figure 2 Time profiles of monthly data of the SSN and inverted intensity of GCR from the Kiel NM. *Blue and red curves* represent an approximation with a polynomial of the fifth degree of SSN data and GCR inverted data, respectively, in the period 1959–1970 for $A < 0$. *Blue and red arrows* show a minimum value of SSN and GCR inverted data, respectively. The *interval between the arrows* represents a DT.

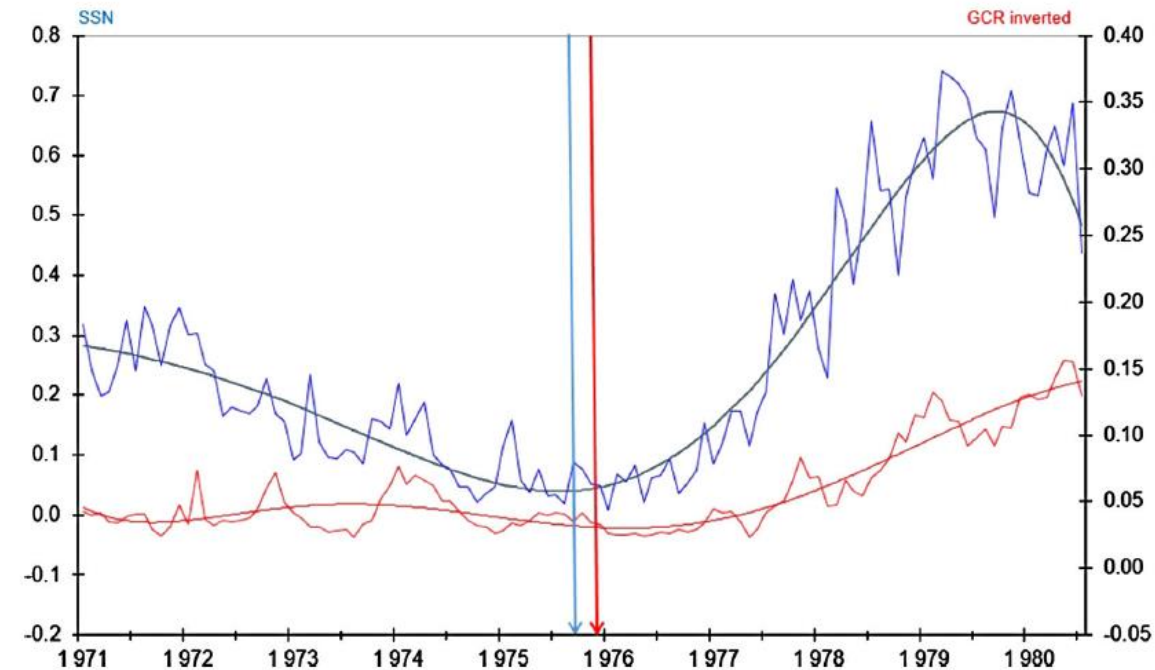
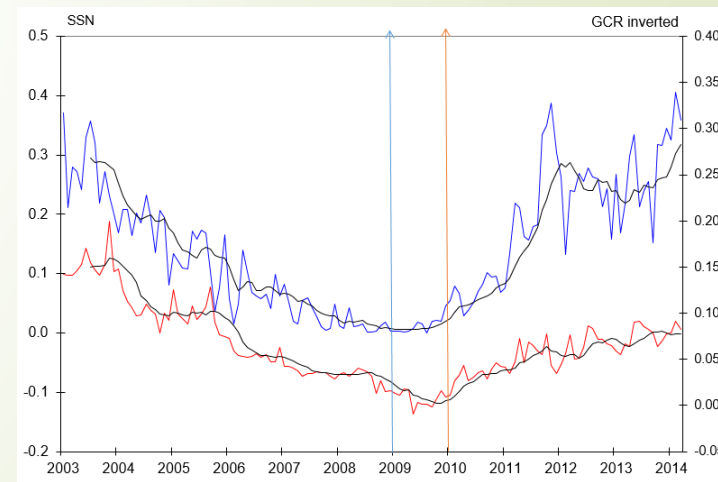
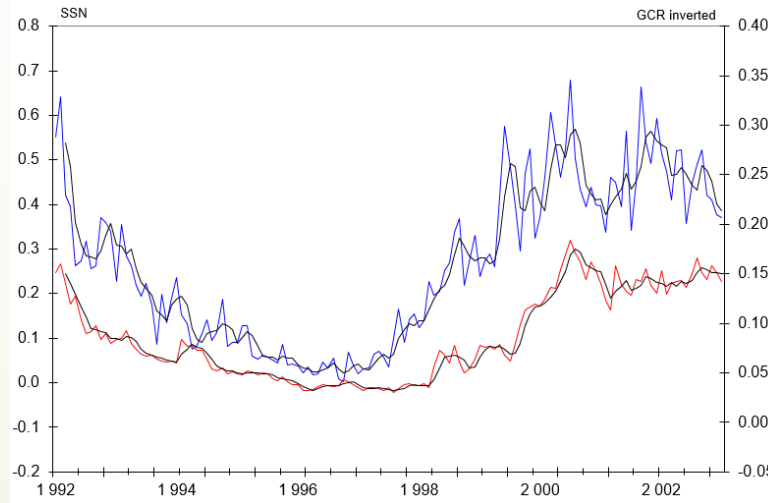
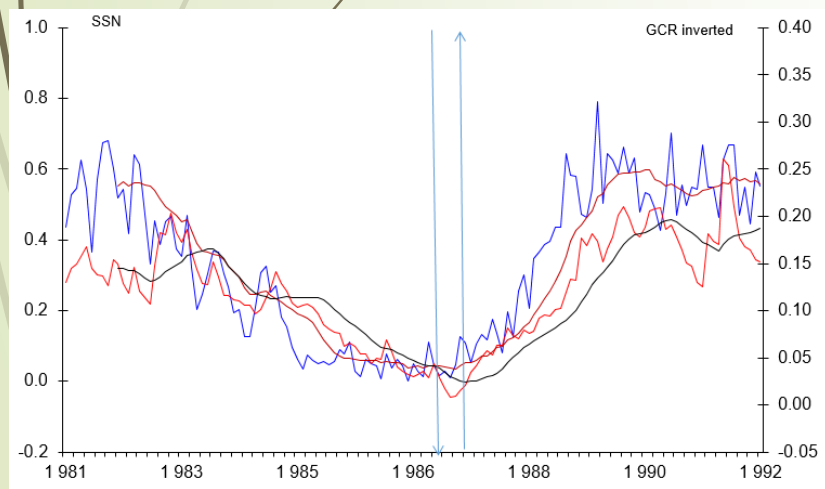
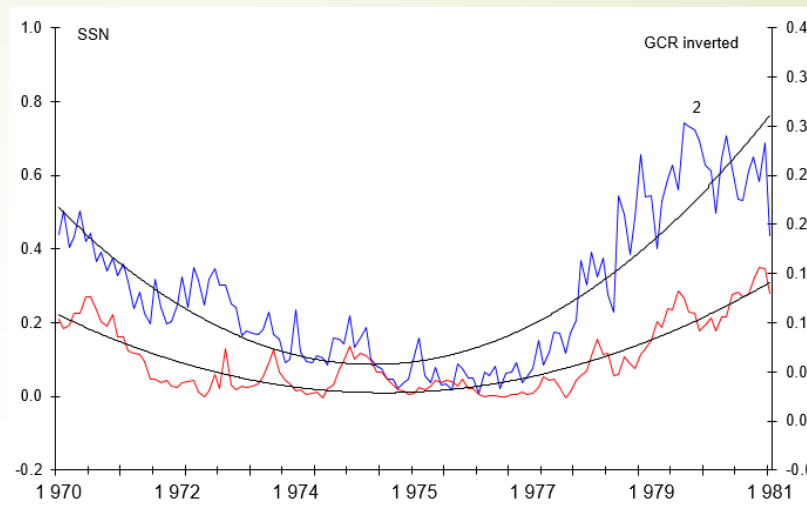
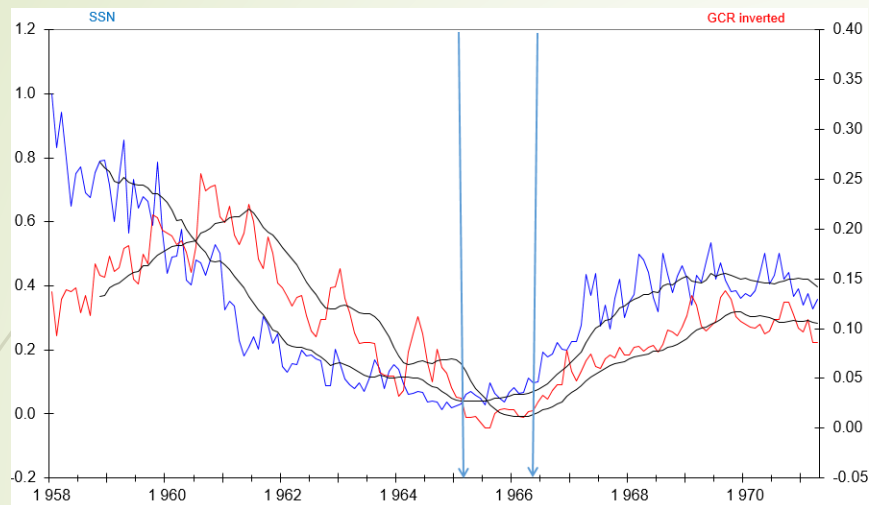


Figure 3 Similar to Figure 2 in the 1971–1979 period for $A > 0$.

On figures are presented time profiles of the monthly data of the sunspot number and inverted intensity of GCR for Kiel neutron monitor in a given sub-periods result of correlation coefficient for above sub-periods

19



Figures
Time profile of the monthly data of the sunspot number and inverted intensity of GCR for Kiel neutron monitor

Table 2 Correlation coefficients and DTs for six pairs of parameters among four of them in five periods

No	Period	Cycles	$r(\text{SSN}, I_{\text{GCR}})$	DT (SSN, I_{GCR}) [months]	$r(\text{SSN}, B)$	DT (SSN, B) [months]	$r(\text{SSN}, \text{TA})$	DT (SSN, TA) [months]	$r(B, I_{\text{GCR}})$	DT (B, I_{GCR}) [months]	$r(B, \text{TA})$	DT (B, TA) [months]	$r(\text{TA}, \text{GCR})$	DT (TA, GCR) [months]
I	1959.00–1969.42	$A < 0$	-0.89	15–17	–	–	–	–	–	–	–	–	–	–
II	1971.58–1979.83	$A > 0$	-0.84	2–0	0.73	0	–	–	-0.81	2	–	–	–	–
III	1980.33–1990.00	$A < 0$	-0.90	6	0.81	4	0.89	-1	-0.83	1	0.75	-9	-0.93	5
IV	1991.33–1999.67	$A > 0$	-0.94	4	0.91	2	0.91	-7	-0.91	1	0.88	-12	-0.96	12
V	2000.42–2012.33	$A < 0$	-0.94	13–14	0.90	13	0.78	-12	-0.96	0	0.74	-17	-0.60	16

Table 3 Correlation coefficients, r , and DTs for 10 sub-periods. In the cycles column, *upward and downward arrows* represent ascending and descending GCR intensity, respectively (see text and Table 2).

No	Period	Cycles	$r(\text{SSN}, I_{\text{GCR}})$	DT (SSN, I_{GCR}) [months]	$r(\text{SSN}, B)$	DT (SSN, B) [months]	$r(\text{SSN}, \text{TA})$	DT (SSN, TA) [months]	$r(B, I_{\text{GCR}})$	DT (B, I_{GCR}) [months]	$r(B, \text{TA})$	DT (B, TA) [months]	$r(\text{TA}, \text{GCR})$	DT (TA, GCR) [months]
1	1959–1965	19 $A < 0 \nearrow$	0.91	15–16	–	–	–	–	–	–	–	–	–	–
2	1965–1968	20 $A < 0 \searrow$	0.88	5	–	–	–	–	–	–	–	–	–	–
3	1971–1976	$\nearrow A > 0$	0.40	0	0.46	–	–	–	-0.53	1	–	–	–	–
4	1976–1978	21 $\searrow A > 0$	0.84	1	0.86	1	0.98	0	-0.92	0	0.87	13	-0.93	3
5	1981–1987	$A < 0 \nearrow$	0.87	10–11	0.84	5	0.90	4	-0.81	0	0.86	-2	-0.93	4
6	1987–1988	22 $A < 0 \searrow$	0.96	4–5	0.88	-7	0.97	0	-0.68	0	0.94	17	-0.97	10
7	1991–1997	$\nearrow A > 0$	0.92	0	0.96	2	0.96	-13	-0.88	0	0.91	-14	-0.97	5
8	1997–1999	23 $\searrow A > 0$	0.86	4–5	0.91	-9	0.93	-1	-0.80	1	0.72	8	-0.97	12
9	2002–2009	$A < 0 \nearrow$	0.93	13–14	0.93	13	0.91	2	-0.94	0	0.95	-4	-0.94	3
10	2009–2013	24 $A < 0 \searrow$	0.80	1	0.85	-5	0.92	-11	-0.84	1	0.86	-4	-0.89	5

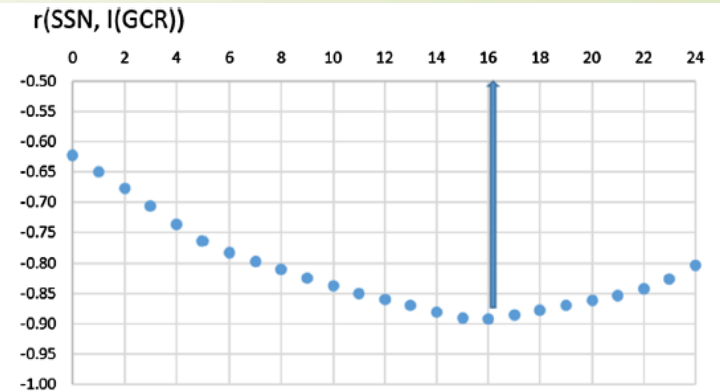
No	Period	Cycles	$r(SSN ; I_{GCR})$	dR	$d(SSN ; I_{GCR})$ [months]
I	1959-1965	$A < 0 \nearrow$	0.91	0.03	15--16
II	1965-1968	$A < 0 \searrow$	0.88	0.05	5
III	1971-1976	$\nearrow A > 0$	0.40	0.08	0
IV	1976-1978	$\searrow A > 0$	0.84	0.06	1
V	1981-1987	$A < 0 \nearrow$	0.87	0.04	10--11
VI	1987-1988	$A < 0 \searrow$	0.96	0.04	4--5
VII	1991-1997	$\nearrow A > 0$	0.92	0.03	0
VIII	1997-1999	$\searrow A > 0$	0.86	0.06	4--5
IX	2002-2009	$A < 0 \nearrow$	0.93	0.03	13--14
X	2009-2013	$A < 0 \searrow$	0.80	0.06	1

Table 2. Coefficients correlation and delay times of different 10 (ascending and descending of GCR intensity or descending and ascending of SA) parts periods of solar magnetic cycles.

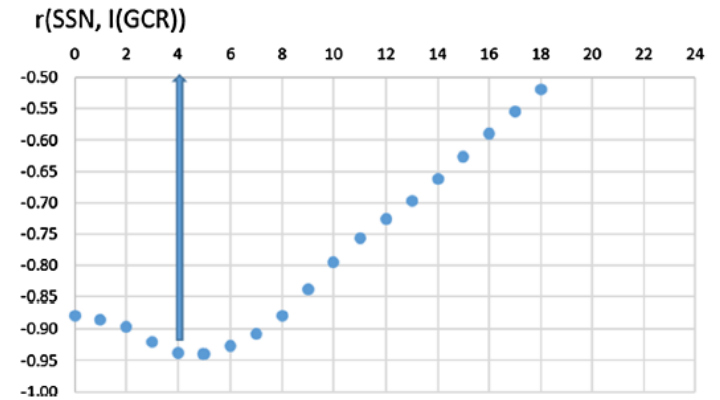
For a examination of the delay time calculated the correlation coefficient between GCR intensity an sunspot number in subsequent five periods depending on the HMF sign.

CONCLUSIONS:

1. Solar activity characterized by the global sunspot number (SSN) and its change determines the conditions prevailing in the heliosphere, *i.e.* variable IMF and its turbulence, HCS, CME, MIR, shocks. These changing conditions affect the GCR propagation in the heliosphere.
2. The structure of the IMF turbulence significantly changes from the minimum to the maximum epoch of SA and shows polarity dependence.
3. A 22-year variation of the DT between SSN and $I(\text{GCR})$ was observed. DTs for periods $A < 0$ are greater than DTs for periods $A > 0$.
4. We also found that DTs in the $A < 0$ epoch are larger in the ascending $I(\text{GCR})$ period than in the descending $I(\text{GCR})$ period. In the $A > 0$ epoch, we did not find DTs in the ascending $I(\text{GCR})$ period, but small DTs in the descending $I(\text{GCR})$ period.
5. The main reasons for this phenomenon are essential temporal rearrangements of the structure of the IMF turbulence. The drift of GCRs caused by the gradient and curvature of the IMF is an additional factor, which strengthens this phenomenon.
6. To establish the properties of DTs from various cycles of SA, it is very important to model and experimentally analyze the propagation of cosmic ray particles in the heliosphere.



(a)



(b)

Figure 7 Correlation coefficients, r , for different monthly shifts (0–24). Up-arrows show DTs obtained from the maximum absolute value of r for periods (see text): (a) 1959–1969 ($A < 0$) DT = (16 ± 1) months. (b) 1991–1999 ($A > 0$) DT = (4 ± 1) months.



THANK YOU

Contact:

marek.siluszyk@uph.edu.pl